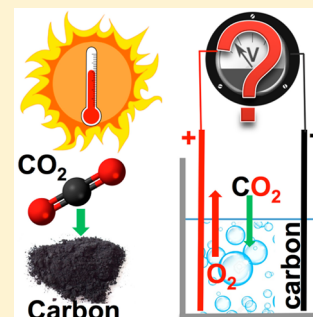


The Minimum Electrolytic Energy Needed To Convert Carbon Dioxide to Carbon by Electrolysis in Carbonate Melts

Jiawen Ren, Jason Lau, Matthew Lefler, and Stuart Licht*

Department of Chemistry, The George Washington University, Washington, D.C. 20052, United States

ABSTRACT: One pathway to remove the greenhouse gas carbon dioxide to mitigate climate change is by dissolution and electrolysis in molten carbonate to produce stable, solid carbon. This study determines critical knowledge to minimize the required electrolysis energy, the reaction stoichiometry in which carbon and O₂ are the principal products, and that CO₂ can be electrolyzed inexpensively. Thermochemical and experimental results indicate that the principal carbon-deposition reaction in molten Li₂CO₃ or Li₂O/Li₂CO₃ electrolytes at 750 °C is Li₂O + 2CO₂ → Li₂CO₃ + C + O₂. The reaction occurs at high Faradaic efficiency of the 4e⁻ reduction of CO₂ to carbon and oxygen at an electrolysis voltage as low as <1 V. Electrolytes without lithium carbonate but containing calcium and/or barium carbonate can also be employed as reaction media for successful carbon deposition, e.g. in an Na/BaCO₃ melt. However, the electrolysis reduction in pure Na or K or Na/K carbonate eutectics at 1 atm of CO₂ forms metals and/or gases, i.e., CO.



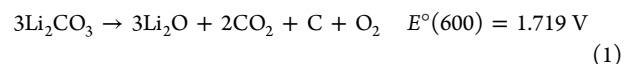
1. INTRODUCTION

A recent report on the future of carbon dioxide (CO₂) emission forecasts that from 2010 to 2060 approximately 496 gigatons of CO₂ will be generated by fossil fuel combustion.¹ Pathways to avoid this emission are sought (i) to avoid the related greenhouse gas effects and their substantial climate change consequences and (ii) to preserve this carbon in a compact, energetic form as a resource for the future. One such pathway is the electrolytic or photochemical reduction of carbon dioxide to more energetic products. At low temperatures ($T < 150$ °C) the Faraday efficiency of the conversion of CO₂ to CO, formates, or other hydrocarbons is low.^{2–6} However, at high temperatures, carbonate melts can be directly reduced into solid carbon or gaseous carbon monoxide products with high Coulombic efficiency.^{7–17} Rather than CO₂ dissolution and splitting conditions for carbon monoxide formation, here we focus on conditions of solid carbon formation as this latter product can be a stable repository to remove CO₂ from the atmosphere. The reversible reduction of carbonates to solid carbon also provides the basis of a new rechargeable molten carbonate air battery¹⁸ as well as a pathway to mitigate the greenhouse gas carbon dioxide by its dissolution and renewable energy electrolysis in molten carbonates.¹⁹ In 2002 and 2003, we presented the theory and experiment of efficient electrolytic water splitting using the full solar spectrum,^{20,21} and in 2009 we extended this theory to carbon dioxide and other electrolyses.¹⁹ The theory, and in 2010 the experimental verification, of STEP carbon (the solar thermal electrochemical process to form carbon),^{12,13,17} utilizes sunlight both as heat and/or as an electric source, to capture and reduce CO₂ into value-added products from molten carbonate electrolytes at high solar efficiency. STEP is an alternative solar energy conversion process, which uses the full spectrum of sunlight, including the sub-bandgap (IR) spectrum, which is not accessible to solar cells, to lower the energy and facilitate the kinetics of useful

endothermic chemical reactions. Iron, cement, ammonia, carbon, and fuels can be readily produced by STEP.^{22–28}

Lithium carbonate, Li₂CO₃, melts at 723 °C, Na₂CO₃ melts at 851 °C, and K₂CO₃ melts at 891 °C. Alkali carbonate mixes melt at lower temperature, and the Li_xNa_yK_zCO₃ eutectic melts at 399 °C. Whereas solid carbon is readily formed by electrolysis in lithium carbonate and a lithium/barium carbonate mix,¹³ the difficulty to form solid carbon by electrolysis from Na₂CO₃ or K₂CO₃, or a mix of the two, has been documented, and instead the alkali metal is the preferred reduction product.^{7,29}

Minimization of the carbonate electrolysis voltage is important to determine the least energy needed to remove carbon dioxide by electrolysis. Recently, Ijije et al. determined thermodynamic potentials for carbon deposition from molten carbonate electrolytes, calculating that the minimum thermodynamic voltage for carbon deposition was over 1.7 V, and the full cell electrolysis potential was very high, i.e., >3.0 V with SnO₂ as the anode.³⁰ At 600 °C an electrolysis potential of 1.719 V to the carbon product was calculated from the standard thermodynamic potential of the reaction²¹



In this study we show carbonate electrolysis pathways in which the solid carbon product is obtained at less than 1.0 V, an alternative stoichiometry for the reaction, and the role of CO₂ and oxide in the formation of the carbon product.

Received: July 20, 2015

Revised: September 18, 2015

Published: October 2, 2015

2. METHODOLOGY

2.1. Calculations. The standard potentials of the reactions are calculated based on eq 2. These data are full thermodynamic cell potentials for the electrolysis (and are not half-reactions). In eq 2, $\Delta G^\circ(T)$ is the Gibbs free energy change of a reaction at temperature (K), and at unit activity, n , E° , and F represent the number of electrons transferred, the cell potential, at unit activity, and the Faraday constant (96 485 C/mol), respectively.

$$\Delta G^\circ(T) = nFE^\circ; \quad \Delta G(T) = \Delta H(T) - T\Delta S(T) \quad (2)$$

In order to investigate the influence of CO_2 pressure, we also calculated the cell potential change if CO_2 pressure is varied from unit activity. The calculations were based on the Nernst equation assuming other species remained at unit activity, in which E and E° represent final and standard cell voltage, respectively. R , T , and Q are the universal gas constant, temperature (K), and reaction quotient.

$$E = E^\circ - RT \ln Q/nF \quad (3)$$

When calculating the decomposition equilibrium, eq 4 is used:

$$\Delta G^\circ = -RT \ln K \quad (4)$$

2.2. Experimental Details. A fired alumina crucible (Al_2O_3 , ceramic, 100 mL capacity) with 65 g of electrolyte was put into an oven and then heated to the target temperature. A cathode (99.9% steel (or platinum yielding the same potential) wire, 0.12 cm diameter, 1.5 cm length exposed to electrolyte) and anode (99.7% iridium foil, 1.0 mm thick, area 25 mm \times 25 mm from Alfa Aesar) were immersed into the electrolyte. A current was applied, and the electrolysis voltage as a function of applied current was monitored by National Instruments Data Acquisition with Lab View software. Note on the alumina crucible stability: From the thermodynamic perspective, we have previously demonstrated that the solubility of LiAlO_2 in molten Li_2CO_3 is 5 *m* at 750 $^\circ\text{C}$ increasing to 12 *m* at 950 $^\circ\text{C}$.¹⁵ From the kinetic perspective, with respect to a molten lithium carbonate electrolyte, we observed that the fired alumina crucible is kinetically stable under conditions of low temperature and low concentrations of lithium oxide and kinetically not stable under conditions of high temperature and high concentrations of lithium oxide. Specifically, at a high temperature of 950 $^\circ\text{C}$, Li_2CO_3 containing 4 *m* (molal, moles per kg of Li_2CO_3) Li_2O will dissolve through the bottom of the alumina crucible within 2 h, while an alumina crucible can contain 750 $^\circ\text{C}$ Li_2CO_3 for tens of hours of electrolysis and (upon cleaning of the crucible) for repeat electrolyses without any measured mass loss or any signs of etching. High concentrations of neither aluminates or silicates are present in the electrolytes of this study. However, we have previously noted that high concentrations of aluminates or silicates increase the observed carbonate electrolyte viscosity but do not significantly influence the observed electrolysis potential.¹⁵

Barium carbonate (Alfa Aesar, 99%), lithium carbonate (Alfa Aesar, 99%), lithium oxide (Alfa Aesar, 99.5%), sodium carbonate (Alfa Aesar, 99%), and potassium carbonate (Alfa Aesar, 99.5%) are used in the electrolysis and solubility studies. Replicate measurements of the lithium carbonate equilibrium were performed with 99.9995%.

The electrolyte composition: $\text{Li}_2\text{CO}_3/\text{Na}_2\text{CO}_3$ contains 55.3 mol % Li_2CO_3 , $\text{Li}_2\text{CO}_3/\text{BaCO}_3$ contains 65 mol % Li_2CO_3 , and $\text{Na}_2\text{CO}_3/\text{BaCO}_3$ contains 30.9 mol % BaCO_3 .

3. RESULTS AND DISCUSSION

The equilibrium for carbonates to decompose to carbon dioxide and oxides, or to form carbonate from them in the reverse reaction, is given by



A thermodynamic comparison of the stability of carbonates at temperatures in which the electrolytic formation of solid carbon is observed ($T < 900$ $^\circ\text{C}$) indicates that the release of CO_2 is unlikely during lithium carbonate electrolysis. To the contrary, CO_2 can be easily absorbed by melts or corresponding oxides.³¹ This is in contradiction to eq 1. K_{MCO_3} is calculated from the thermochemical free energies for a variety of alkali and alkali earth carbonates (where $M = \text{Li}, \text{Na}, \text{K}, \text{Mg}, \text{Ca}$, or Ba) and plotted as a function of temperature in Figure 1. Thermochem-

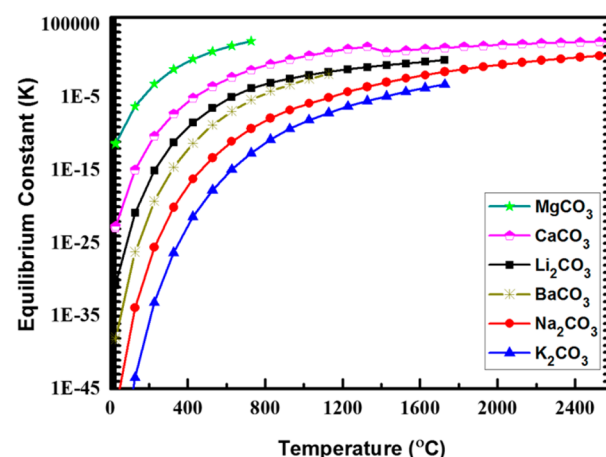


Figure 1. Comparison of the equilibrium constant, K_{MCO_3} , for carbonate decomposition as calculated from the thermochemistry of the carbonate, carbon dioxide, and oxide components. Regarding the CaCO_3 discontinuity at 1200–1300 $^\circ\text{C}$, solid argonite decomposes at 825 $^\circ\text{C}$, while calcite melts at 1339 $^\circ\text{C}$.

ical values of oxides and carbonates^{32,33} and the calculated decomposition free energies are compiled in Tables 1–3. Above each carbonate decomposition equilibrium curve in Figure 1, CO_2 will react spontaneously with the metal oxide to form the metal carbonate, and below the curve the metal carbonate will decompose, releasing CO_2 . As is evident in the figure, MgCO_3 is the least stable of the indicated carbonates, followed by CaCO_3 whose solid decomposition at ~ 850 $^\circ\text{C}$ is the basis of lime (CaO) production from limestone. Na_2CO_3 and K_2CO_3 are the most stable, while lithium and barium carbonates are highly stable with low K_{MCO_3} values in the temperature window of 400–800 $^\circ\text{C}$, which is a typical range for the electrolysis of carbonate melts to form carbon. For example, at 900 K (623 $^\circ\text{C}$), the equilibrium constants of decomposition of carbonates are in turn MgCO_3 (143.47) > CaCO_3 (6.7×10^{-3}) > Li_2CO_3 (1.27×10^{-5}) > BaCO_3 (1.08×10^{-7}) > Na_2CO_3 (9.50×10^{-12}) > K_2CO_3 (1.39×10^{-15}). At 750 $^\circ\text{C}$, $K_{\text{Li}_2\text{CO}_3}$ calculated from the thermochemical free energy is 3.0×10^{-4} . Each of the equilibrium constants in Figure 1 is calculated to include a thermodynamic equilibrium activity of carbonate, oxide, and carbon dioxide. As we have previously reported, the solubility of the oxide can be high (such as for lithium or barium oxide)^{13,24} or low (such as for calcium oxide)

Table 1. Gibbs Free Energy (kJ/mol) of Pure Carbonates at Different Temperatures

T/K	T/°C	Li ₂ CO ₃ ^a	Na ₂ CO ₃ ^a	K ₂ CO ₃ ^a	MgCO ₃ ^a	CaCO ₃ ^a	BaCO ₃ ^b
298	25	−1242.901	−1172.130	−1196.525	−1131.315	−1233.943	−1137.653
300	27	−1243.082	−1172.408	−1196.836	−1131.447	−1234.113	−1137.165
400	127	−1253.705	−1188.097	−1214.251	−1139.300	−1244.673	−1110.904
500	227	−1267.155	−1206.938	−1234.896	−1149.404	−1257.662	−1084.834
600	327	−1283.200	−1228.636	−1258.350	−1161.516	−1272.747	−1058.799
700	427	−1301.730	−1253.063	−1284.317	−1175.446	−1289.669	−1032.847
800	527	−1322.832	−1280.033	−1312.579	−1191.038	−1308.225	−1007.052
900	627	−1345.922	−1308.966	−1342.969	−1208.161	−1328.257	−981.423
1000	727	−1371.336	−1339.747	−1375.356	−1226.703	−1349.639	−956.000
1100	827	−1402.768	−1372.321	−1409.635		−1372.268	−930.377
1200	927	−1435.888	−1408.648	−1446.328		−1396.058	−906.325
1300	1027	−1470.555	−1447.170	−1486.495		−1420.937	−882.741
1400	1127	−1506.650	−1487.150	−1528.272		−1446.846	−859.576
1500	1227	−1544.070	−1528.486	−1571.546		−1473.729	−1137.653
1600	1327	−1582.728	−1571.086	−1616.214		−1501.541	
1700	1427	−1622.545	−1614.871	−1662.192		−1564.405	
1800	1527	−1663.454	−1659.772	−1709.400		−1597.231	
1900	1627	−1705.393	−1705.727	−1757.771		−1630.900	
2000	1727	−1748.309	−1752.679	−1807.244		−1665.368	
2100	1827		−1800.580	−1857.763		−1700.599	
2200	1927		−1849.383	−1909.279		−1736.557	
2300	2027		−1899.049	−1961.746		−1773.212	
2400	2127		−1949.538	−2015.123		−1810.535	
2500	2227		−2000.818	−2069.372		−1848.495	
2600	2327		−2052.856			−1887.071	
2700	2427		−2105.623			−1926.241	
2800	2527		−2159.092			−1965.984	
2900	2627		−2213.238			−2006.276	
3000	2727		−2268.038			−2006.276	

^aCalculated based on enthalpy and entropy data from ref 24. ^bCalculated based on enthalpy and entropy data from ref 23.

in these carbonates.²⁶ In the case where the solubility of the oxide is higher than the equilibrium activity of the oxide, then the equilibrium state is a carbonate solution containing dissolved oxide. In the case where the solubility of the oxide is less than the equilibrium activity of the oxide, then the equilibrium state will be the decomposition of the carbonate, resulting in the solid oxide (and released carbon dioxide). Such is the case for the common industrial formation of lime (CaO) from limestone (CaCO₃) in which solid limestone is heated, releasing CO₂ to form the desired CaO product.²⁵

Experimentally, we estimate $K_{\text{Li}_2\text{CO}_3}$ by mass loss or mass gain of the molten carbonate. Li₂CO₃ heated to 750 °C in air (containing $p_{\text{CO}_2} = 4.0 \times 10^{-4}$ atm of CO₂) evolves 0.018 mole fraction of CO₂. The mass loss is equivalent to the equilibrium formation of 0.25 *m* Li₂O ($m \equiv \text{molal} = \text{mol kg}^{-1} \text{Li}_2\text{CO}_3$) determined as $0.018 / ((1 - 0.018) \times 0.07391) \text{ kg mol}^{-1} \text{Li}_2\text{CO}_3$ in the molten lithium carbonate. However, this is regarded as a lower bound of this value to the equilibrium concentration at 750 °C value, as it does not include any initial Li₂O impurities in the Li₂CO₃. pH titration by HCl of the original Li₂CO₃ dissolved as an aqueous solution indicates any Li₂O impurity is <1% of the total carbonate. In accord with the reverse reaction of eq 5, when Li₂O is added to the carbonate, the 750 °C Li₂CO₃ is observed to gain, rather than lose, mass, that is, absorb CO₂ from air. We measure that a mix of 0.51 *m* Li₂O in Li₂CO₃ heated to 750 °C gains mass equivalent to the absorption of 0.18 *m* CO₂, for a final concentration of 0.33 *m* Li₂O in solution.

From the upper and lower bound measurements, the equilibrium concentration of Li₂O in molten lithium carbonate at 750 °C is $0.29 \pm 0.04 \text{ m}$. This yields an experimental value of the 750 °C equilibrium constant of $K_{\text{MCO}_3} = 4.0 \times 10^{-4} \times 0.29 = 1.2 \times 10^{-4}$, which is similar to, but lower than, the 3.0×10^{-4} thermochemical value. While the thermochemistry of the solid alkali and alkali earth oxides has been well characterized^{32,33} (and is used in our equilibrium calculations), the solvation energy of oxides in carbonates has not. At higher temperatures (above 800 °C) for lithium carbonate, the variation between the measured and calculated K_{MCO_3} had been attributed to the free energy difference between the solid and the dissolved oxide.³⁴ The differences between our measured and calculated K_{MCO_3} for Li₂CO₃ at 750 °C are equivalent to a small solvation energy difference of 7.8 kJ/mol, but we note that a portion of this difference may also be attributed to the unknown activity coefficients of Li₂O and CO₂ in molten Li₂CO₃.

We have observed that solid carbon is the sole carbon containing product when lithium carbonate is electrolyzed at 750 °C.^{12,17} The carbon product is a mix of solid carbon and carbon monoxide at 850 °C, and carbon monoxide is the sole product at 950 °C.^{11,12} It is evident from these measurements, and from the thermodynamic equilibria, that at the temperature range in which lithium carbonate can be electrolyzed to form a solid carbon product molten lithium carbonate in contact with air will spontaneously form a low equilibrium concentration of dissolved lithium oxide and that at higher concentrations the lithium carbonate will spontaneously absorb, rather than emit,

Table 2. Gibbs Free Energy (kJ/mol) of Relevant Oxides at Different Temperatures

T/K	CO ₂ ^a	Li ₂ O ^a	Na ₂ O ^a	K ₂ O ^a	MgO ^a	CaO ^a	BaO ^b	CO ₂ ^b
298	−457.234	−610.028	−440.344	−391.231	−609.264	−646.478	−525.346	−394.364
300	−457.662	−610.104	−440.495	−391.420	−609.317	−646.554	−525.171	−394.37
400	−479.646	−614.796	−449.118	−402.191	−612.619	−651.062	−515.784	−394.646
500	−502.668	−621.089	−459.648	−415.261	−616.992	−656.741	−506.435	−394.903
600	−526.586	−628.778	−471.812	−430.229	−622.282	−663.405	−496.941	−395.139
700	−551.295	−637.701	−485.408	−446.806	−628.365	−670.913	−487.344	−395.347
800	−576.712	−647.730	−500.276	−464.851	−635.145	−679.160	−477.709	−395.527
900	−602.774	−658.769	−516.288	−484.216	−642.547	−688.062	−468.034	−395.68
1000	−629.426	−670.736	−533.337	−504.798	−650.510	−697.555	−458.342	−395.81
1100	−656.620	−683.566	−551.442	−526.517		−707.586	−447.872	−395.918
1200	−684.320	−697.205	−570.487	−549.305		−718.111	−437.371	−396.007
1300	−712.485	−711.603	−590.889	−573.108		−729.094	−426.868	−396.079
1400	−741.093	−726.718	−612.468	−597.877		−740.502	−416.372	−396.136
1500	−770.115	−742.511	−638.032	−623.573		−752.309	−405.886	−396.179
1600	−799.526	−758.947	−664.434	−650.162		−764.492	−395.413	−396.21
1700	−829.305	−775.977	−691.489	−677.612		−777.030	−384.958	−396.229
1800	−859.434	−793.598	−719.160	−705.897		−789.904	−374.518	−396.237
1900	−889.894	−813.583	−747.413	−734.994		−803.098	−364.100	−396.235
2000	−920.670	−835.464	−776.216	−764.880		−816.598	−353.705	
2100	−951.748		−805.543			−830.391		
2200	−983.115		−835.368			−844.464		
2300	−1014.759		−865.668			−858.807		
2400	−1046.668		−896.424			−873.410		
2500	−1078.832		−927.615			−888.263		
2600	−1111.243		−959.225			−903.359		
2700	−1143.890		−991.237			−918.690		
2800	−1176.767		−1023.637			−934.247		
2900	−1209.865		−1056.411			−950.026		
3000	−1243.177		−1089.545			−966.019		

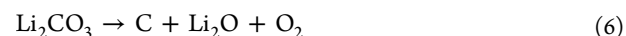
^aCalculated based on enthalpy and entropy data from ref 24. ^bCalculated based on enthalpy and entropy data from ref 23.

CO₂. Lubomirsky and co-workers have experimentally measured the lithium oxide in lithium carbonate equilibrium³⁴ with a focus on the higher temperature domain of relevance to the electrolytic formation of carbon monoxide,¹¹ rather than the electrolytic formation of solid carbon which is the focus of this study. The temperature range measured by Lubomirsky et al. was 800–975 °C, and the highest lithium oxide concentration measured in that study was 0.06 mole fraction.

We have previously noted that molten Li₂CO₃ is readily electrolyzed between a nickel or iridium anode and a steel or platinum cathode.^{12,17,24} Nickel anodes form a highly stable oxide layer in molten Li₂CO₃, iridium is even more stable as an anode, and steel cathodes are reusable subsequent to removal of the cathode product. When 5 cm² electrodes are immersed in 750 °C Li₂CO₃ and electrolyzed at 1 A for 1 h (1 Ah), a black deposit grows at the cathode and gas is evolved in the vicinity of the anode. Subsequently, the cathode product is cooled and washed to remove excess electrolyte and yields 0.11 g of product. The product is identified as pure carbon by EDS, and the mass is equivalent to 4e[−] (electron) 100% Faradaic conversion of tetravalent carbon, such as in CO₃^{2−} or CO₂, to solid carbon at the cathode. In concurrence with a prior report,¹⁴ CO₂ was not detected in the gas product by gas chromatography (GC).

Figure 2 includes the current–voltage polarization measured for the electrolysis of lithium carbonate at 750 °C. The reduction of lithium is thermodynamically not feasible at the low potentials measured in this study. The formation of carbon as the principal Faradaic product is demonstrated gravimetri-

cally by the high Coulombic efficiency of the carbon (carbon as chemically characterized by XRD and EDS). The Coulombic efficiency is measured by comparing the mass, and hence measured moles of carbon formed, to the current passed during the electrolysis. For the pure Li₂CO₃ electrolyte, the minimum measured electrolysis potential of 1.1 V is considerably less than the thermodynamic potential calculated value of 1.72 V according to eq 1. During the electrolysis oxygen rather than carbon dioxide is the gas evolved. Rather than eq 1, the mass observed and the generation of oxygen initially appear to be consistent with an electrolysis of the molten carbonate of



Furthermore, the presence of BaCO₃ or Na₂CO₃ resulted in a much higher full cell voltage as shown on the right side of Figure 2. In Na₂CO₃/BaCO₃ eutectics, the electrolysis occurs at very high onset potential, i.e. >1.8 V, compared to that observed in lithium carbonate.

The right side of Figure 3 presents the calculated thermodynamic electrochemical full cell potential in lithium carbonate to products which include lithium metal. In this figure, the lowest potential occurs when the product includes both Li and solid carbon. Even that mixed product reaction occurs at potentials considerably higher than for the reactions without a Li metal product on the left figure to reactions. The observations that no lithium metal was obtained during lithium carbonate electrolyses and ~100% Coulombic efficiency toward carbon (*T* < 800 °C) rule out the significant occurrence of the right figure reactions. The left side of Figure 3 includes the

Table 3. Gibbs Free Energy Change, $\Delta G(T)$ (kJ/mol), of the Decomposition Reaction of Carbonate into Oxide and CO_2 with Temperatures: $\text{MCO}_3 \rightarrow \text{MO} + \text{CO}_2$ ($\text{M} = \text{Li}_2, \text{Na}_2, \text{K}_2, \text{Mg}, \text{Ca}, \text{Ba}$)

T/K	$T/^\circ\text{C}$	Li_2CO_3	Na_2CO_3	K_2CO_3	MgCO_3	CaCO_3	BaCO_3
298	25	175.638	274.551	348.059	64.817	130.232	217.943
300	27	175.316	274.251	347.755	64.468	129.897	217.624
400	127	159.263	259.333	332.415	47.036	113.966	200.474
500	227	143.398	244.621	316.966	29.744	98.252	183.496
600	327	127.836	230.238	301.534	12.648	82.756	166.719
700	427	112.735	216.360	286.216	−4.213	67.461	150.156
800	527	98.389	203.044	271.015	−20.819	52.353	133.816
900	627	84.379	189.904	255.979	−37.160	37.421	117.709
1000	727	71.175	176.985	241.132	−53.233	22.658	101.848
1100	827	62.581	164.259	226.498		8.061	86.587
1200	927	54.364	153.842	212.703		−6.373	72.947
1300	1027	46.467	143.795	200.902		−20.642	59.794
1400	1127	38.838	133.588	189.302		−34.750	47.068
1500	1227	31.444	120.338	177.857		−48.695	
1600	1327	24.255	107.126	166.526		−62.477	
1700	1427	17.263	94.077	155.274		−41.930	
1800	1527	10.422	81.178	144.069		−52.106	
1900	1627	1.916	68.420	132.884		−62.092	
2000	1727	−7.825	55.793	121.694		−71.901	
2100	1827		43.288			−81.541	
2200	1927		30.900			−91.023	
2300	2027		18.622			−100.354	
2400	2127		6.447			−109.543	
2500	2227		−5.630			−118.601	
2600	2327		−17.612			−127.531	
2700	2427		−29.505			−136.339	
2800	2527		−41.312			−145.030	
2900	2627		−53.037			−153.614	
3000	2727		−64.683			−202.919	

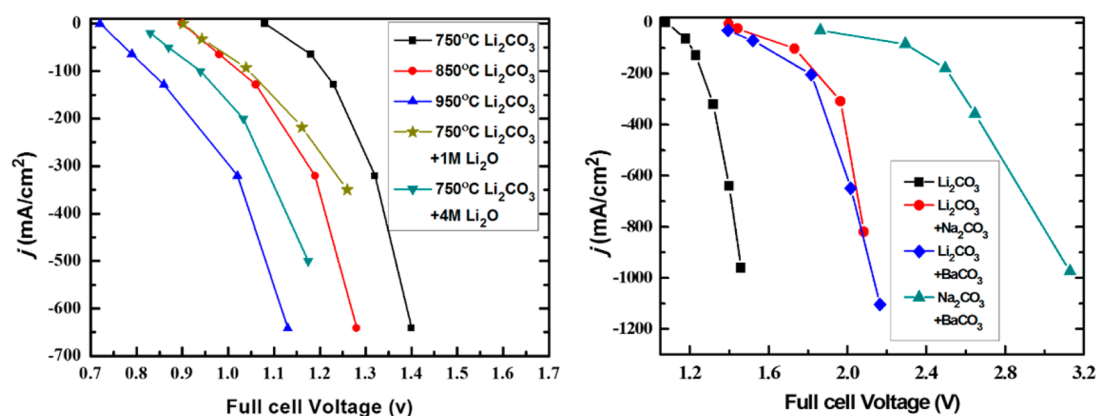


Figure 2. Measured full cell electrolysis potential currents for a range of stable carbon dioxide splitting currents in various electrolytes. Left: polarization curves of full cell voltage for pure Li_2CO_3 at different temperatures and 750 °C with Li_2O involved. Right: full cell electrolysis potential for a range of stable cathodic current densities in different electrolytes at 750 °C.

calculated thermodynamic electrolysis potential for the electrochemical reduction of Li_2CO_3 to either a solid carbon or carbon monoxide product. The lower calculated potential of 1.2 V for eq 6 approaches the 750 °C experimental value of 1.08 V observed in Figure 2. Also consistent with the experimental observation is that the calculated low-energy product shifts from solid carbon (blue curve) to carbon monoxide (red curve) with increasing temperature. The energy minimum in Figure 3 (left) shifts from the solid carbon to carbon monoxide (plus oxygen) product at ~900 °C.

The Li_2CO_3 electrolysis to C, O_2 , and Li_2O (eq 6) determines a lower electrolysis potential than eq 1, is closer to the observed electrolysis potential, and is consistent with the observed electrolysis products. However, as apparent in the experimental measurements in Figure 2, the Li_2CO_3 electrolysis potentials also decrease substantially with added concentrations of lithium oxide, falling to ~0.8 V with 4 m Li_2O dissolved in the Li_2CO_3 at 750 °C. This decrease is not predicted by eq 6. Rather, in eq 6 an increased concentration of product (Li_2O) would result in an increase of the calculated potential. Furthermore, when we bubbled CO_2 into the electrolyte, the

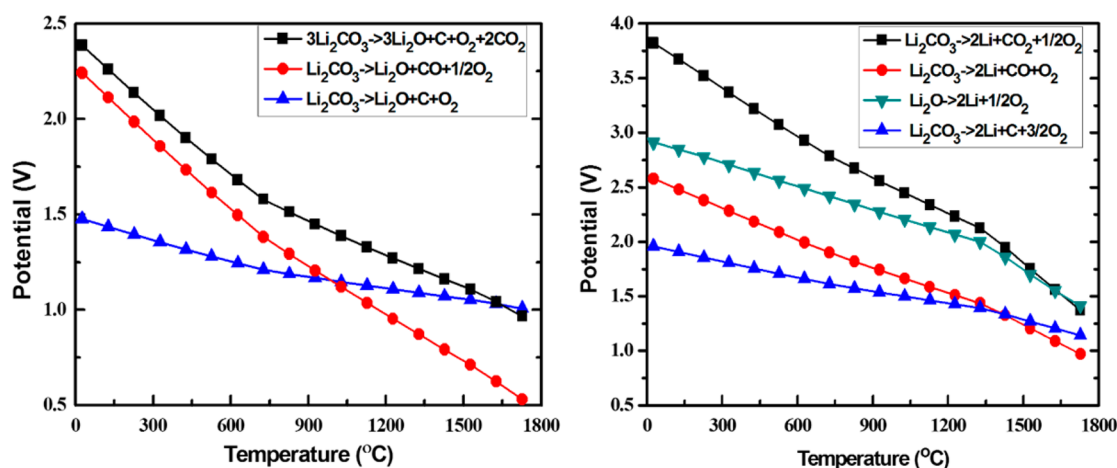


Figure 3. Calculated electrochemical full cell potentials for possible electrolysis reactions related to carbon capture and conversion in Li_2CO_3 . Left: electrolyses to oxides and a carbon/CO product. Right: electrolyses to a lithium metal product.

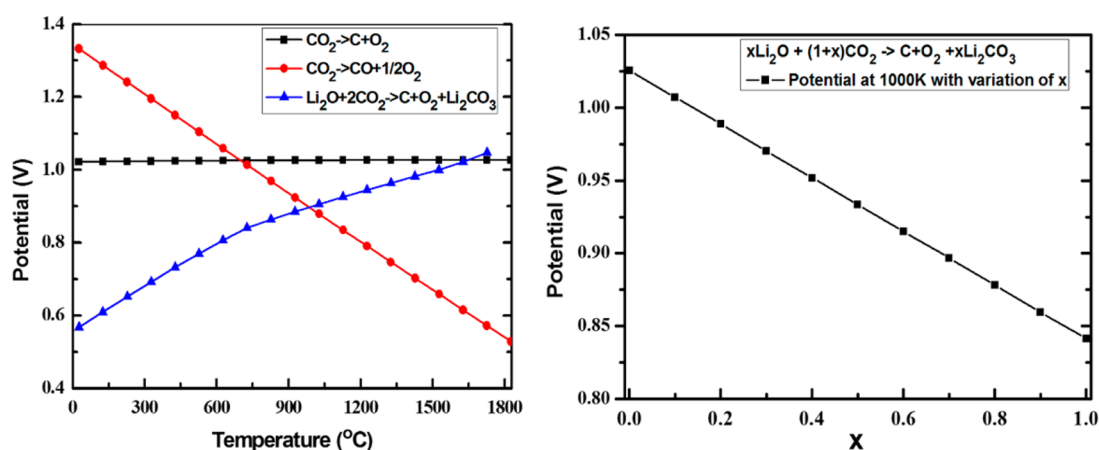
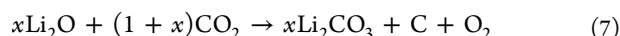


Figure 4. Left: calculated electrochemical full cell potentials for $\text{CO}_2 \rightarrow \text{C} + \text{O}_2$, $\text{CO}_2 \rightarrow \text{CO} + 1/2\text{O}_2$, and $\text{Li}_2\text{O} + 2\text{CO}_2 \rightarrow \text{Li}_2\text{CO}_3 + \text{C} + \text{O}_2$. Right: variation with x of the calculated electrochemical full cell potentials for $x\text{Li}_2\text{O} + (1+x)\text{CO}_2 \rightarrow x\text{Li}_2\text{CO}_3 + \text{C} + \text{O}_2$.

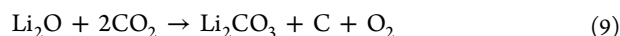
observed voltage is 30–50 mV lower than without bubbling. Both the Li_2O and CO_2 potential decrease are consistent with the addition of multiples of the reverse of eq 5 for the Li carbonate case, which yields



When $x = 0$ the direct reduction of CO_2 occurs



and $x = 1$ represents the reaction



The left side of Figure 4 includes the calculated thermodynamic electrolysis potential for CO_2 splitting (eq 8) and compares this to the combined CO_2 plus Li_2O splitting in eq 9. The right side of the figure includes the intermediate cases that is the variation of eq 7 with increasing x . The case of $x = 1$ is equivalent to unit activity of Li_2O in eq 9. It should be noted that the calculated value of 0.841 at 1000 K (which will decrease by a calculated 0.019 V when including the estimated 7.8 kJ/mol Li_2O solvation energy) is similar to the measured experimental value for the electrolysis of lithium carbonate with 1 *m* Li_2O in Figure 2, and the case of $x = 0$ (0 added Li_2O) compares well with the measured electrochemical potential in pure Li_2CO_3 in Figure 2. We conclude that eq 9 is the

thermodynamically most consistent electrochemical reaction representing the observed experimental electrolysis in lithium carbonate electrolyte to carbon and oxygen. Simultaneously, eq 5, the chemical equilibration of lithium carbonate, yields further Li_2O for continued electrolysis. The net of eqs 5 (when $M = \text{Li}_2$) and 9 is the simple electrolysis of CO_2 to oxygen and carbon, which is consistent with the observed mass of products during the electrolysis.

A solid carbon product can also be produced by electrolysis from electrolytes without lithium salts. Our calculations (not shown) suggest a very low MgCO_3 to carbon electrolysis potential. However, in accord with Figure 1, MgCO_3 will readily decompose unless electrolyzed under high pressure of CO_2 . As previously noted, potassium carbonate will yield solid carbon under high carbon dioxide pressure but tends to form potassium metal under ambient pressures.⁹ High pressure of CO_2 was the key to deposit a carbon product onto cathode during electrolysis of NaCl/KCl eutectics, in accord with the carbon formation reaction eq 8.³⁵ It is interesting to investigate the thermodynamic influence of pressure of CO_2 toward products. The calculation results of CO_2 splitting into carbon or CO are shown in Figure 5. It is noteworthy that the increase of pressure significantly decreases the reaction potential for the reactions, especially toward CO release. This provides a low-

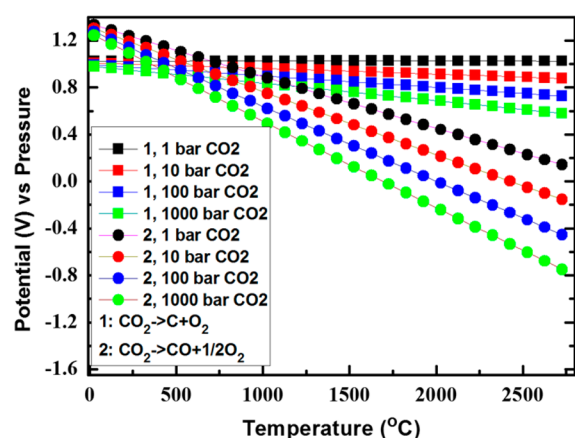


Figure 5. Calculated electrochemical full cell potentials for $\text{CO}_2 \rightarrow \text{C} + \text{O}_2$ and $\text{CO}_2 \rightarrow \text{CO} + \frac{1}{2}\text{O}_2$ with the variation of CO_2 partial pressures.

energy pathway toward CO as a product, one component of syngas.³⁶

A carbon product was observed during electrolysis of BaCO_3 dissolved in a halide (chloride) melt.³⁷ In our lab, Na/K/CaCO_3 and Na/BaCO_3 were utilized as electrolytes, and a carbon electrolysis product is also observed at the cathode as exemplified in Figure 6. The observed reaction in the



Figure 6. Product from the electrolysis of $\text{Na}_2\text{CO}_3/\text{BaCO}_3$ electrolyte.

electrolysis is related to the oxide solubility in the electrolyte.^{38,39} For example, in the Na/K/CaCO_3 system, the reaction could also be $3\text{CO}_3^{2-} \rightarrow \text{C} + 2\text{CO}_2 + \text{O}_2 + 3\text{O}^{2-}$, since CaO has poor solubility,³¹ and the anode will have insufficient O^{2-} to maintain mass transport for the direct O_2 evolution reaction: $\text{O}^{2-} \rightarrow \text{O}_2^{2-} \rightarrow \text{O}_2 \rightarrow \text{O}_2$.

The combined eqs 6 and 7 process provides a Faradaic efficient (approaching 100% Coulombic efficiency for the $4e^-$ reduction of CO_2) and low-energy (occurring at potentials <1 V) process for the conversion of the greenhouse gas carbon dioxide to a compact, storable, and energetic pure carbon product. This means the energy consumption of the electrolysis can be derived as 9.6 kW h per kg C assuming a 95% current efficiency, which can be translated to a cost of less than \$2 per kg C considering a 20% margin for heating and post-treatment. The presence of Li_2O in the molten electrolyte largely reduces the energy needed for the electrolytic deposition of carbon and facilitates CO_2 adsorption into the electrolyte.

AUTHOR INFORMATION

Corresponding Author

*E-mail: slicht@gwu.edu (S.L.).

Notes

The authors declare no competing financial interest.

ACKNOWLEDGMENTS

We are grateful for support of this research by NSF Grant 1230732.

REFERENCES

- (1) Davis, S. J.; Caldeira, K.; Matthews, H. D. Future CO_2 Emissions and Climate Change from Existing Energy Infrastructure. *Science* **2010**, 329, 1330–1333.
- (2) Kumar, B.; Asadi, M.; Pisasale, D.; Sinha-Ray, S.; Rosen, B. A.; Haasch, R.; Abiad, J.; Yarin, A. L.; Salehi-Khojin, A. Renewable and Metal-free Carbon Nanofibre Catalysts for Carbon Dioxide Reduction. *Nat. Commun.* **2013**, 4, 2819.
- (3) Li, C. W.; Kanan, M. W. CO_2 Reduction at Low Overpotential on Cu Electrodes Resulting from the Reduction of Thick Cu_2O Films. *J. Am. Chem. Soc.* **2012**, 134, 7231–7234.
- (4) Richardson, R. D.; Holland, E. J.; Carpenter, B. K. A Renewable Amine for Photochemical Reduction of CO_2 . *Nat. Chem.* **2011**, 3, 301–303.
- (5) Rosen, B. A.; Salehi-Khojin, A.; Thorson, M. R.; Zhu, W.; Whipple, D. T.; Kenis, P. J. A.; Masel, R. I. Ionic Liquid-Mediated Selective Conversion of CO_2 to CO at Low Overpotentials. *Science* **2011**, 334, 643–644.
- (6) Simon-Manso, E.; Kubiak, C. P. Dinuclear Nickel Complexes as Catalysts for Electrochemical Reduction of Carbon Dioxide. *Organometallics* **2005**, 24, 96–102.
- (7) Bartlett, H. E.; Johnson, K. E. Electrolytic Reduction and Ellingham Diagrams for Oxy-anion Systems. *Can. J. Chem.* **1966**, 44, 2119–2129.
- (8) Bartlett, H. E.; Johnson, K. E. Electrochemical Studies in Molten Li_2CO_3 - Na_2CO_3 - K_2CO_3 . *J. Electrochem. Soc.* **1967**, 114, 457–461.
- (9) Shapoval, V. I.; Solov'ev, V. V.; Malyshev, V. V. Electrochemically Active Species and Multielectron Processes in Ionic Melts. *Russ. Chem. Rev.* **2001**, 2, 182–199.
- (10) Kaplan, B.; Groult, H.; Barhoun, A.; Lantelme, F.; Nakajima, T.; Gupta, V.; Komaba, S.; Kumagai, N. Synthesis and Structural Characterization of Carbon Powder by Electrolytic Reduction of Molten Li_2CO_3 - Na_2CO_3 - K_2CO_3 . *J. Electrochem. Soc.* **2002**, 149, D72–D78.
- (11) Kaplan, V.; Wachtel, E.; Gartsman, K.; Feldman, Y.; Lubomirsky, I. Conversion of CO_2 to CO by Electrolysis of Molten Lithium Carbonate. *J. Electrochem. Soc.* **2010**, 157, B552–B556.
- (12) Licht, S.; Wang, B.; Ghosh, S.; Ayub, H.; Jiang, D.; Ganley, J. A New Solar Carbon Capture Process: Solar Thermal Electrochemical Photo (STEP) Carbon Capture. *J. Phys. Chem. Lett.* **2010**, 1, 2363–2368.
- (13) Licht, S.; Cui, B.; Wang, B. STEP Carbon Capture: The Barium Advantage. *J. CO₂ Util.* **2013**, 1, 2363–2368.
- (14) Yin, H.; Mao, X.; Tang, D.; Xiao, W.; Xing, L.; Zhu, H.; Wang, D.; Sadoway, D. R. Capture and Electrochemical Conversion of CO_2 to Value-added Carbon and Oxygen by Molten Salt Electrolysis. *Energy Environ. Sci.* **2013**, 6, 1538–1545.
- (15) Ijije, H. V.; Lawrence, R. C.; Chen, G. Z. Carbon Electrodeposition in Molten Salts: Electrode Reactions and Applications. *RSC Adv.* **2014**, 4, 35808–35817.
- (16) Ijije, H. V.; Sun, C.; Chen, G. Z. Indirect Electrochemical Reduction of Carbon Dioxide to Carbon Nanopowders in Molten Alkali Carbonates: Process Variables and Product Properties. *Carbon* **2014**, 73, 163–174.
- (17) Ren, J.; Li, F.-F.; Lsu, J.; Gonzalez-Urbina, L.; Licht, S. One-pot Synthesis of Carbon Nanofibers from CO_2 . *Nano Lett.* **2015**, 15, 6142–6148.
- (18) Licht, S.; Cui, B.; Stuart, J.; Wang, B.; Lau, J. Molten Air - A New, Highest Energy Class of Rechargeable Batteries. *Energy Environ. Sci.* **2013**, 6, 3646–3657.

- (19) Licht, S. STEP (Solar Thermal Electrochemical Photo) Generation of Energetic Molecules: A Solar Chemical Process to End Anthropogenic Global Warming. *J. Phys. Chem. C* **2009**, *113*, 16283–16292.
- (20) Licht, S. STEP-A Solar Water Splitting to Generate Hydrogen Fuel: Photothermal Electrochemical Analysis. *J. Phys. Chem. B* **2003**, *107*, 4253–4260.
- (21) Licht, S.; Halperin, L.; Kalina, M.; Zidman, M.; Halperin, N. Electrochemical Tuned Water Splitting. *Chem. Commun.* **2003**, 3006–3007.
- (22) Licht, S. Efficient Solar-Driven Synthesis, Carbon Capture, and Desalinization, STEP: Solar Thermal Electrochemical Production of Fuels, Metals, Bleach. *Adv. Mater.* **2011**, *23*, 5592–5612.
- (23) Licht, S.; Wang, B. High Solubility Pathway for the Carbon Dioxide Free Production of Iron. *Chem. Commun.* **2010**, *46*, 7004–7006.
- (24) Licht, S.; Wu, H. STEP Iron, a Chemistry of Iron Formation without CO₂ Emission: Molten Carbonate Solubility and Electrochemistry of Iron Ore Impurities. *J. Phys. Chem. C* **2011**, *115*, 25138–25147.
- (25) Cui, B.; Licht, S. Critical STEP Advances for Sustainable Iron Production. *Green Chem.* **2013**, *15*, 881–884.
- (26) Licht, S.; Wu, H.; Hettige, C.; Wang, B.; Lau, J.; Asercion, J.; Stuart, J. STEP Cement: Solar Thermal Electrochemical Production of CaO Without CO₂ Emission. *Chem. Commun.* **2012**, *48*, 6019–6021.
- (27) Licht, S.; Cui, B.; Wang, B.; Li, F.; Lau, J.; Liu, S. Ammonia Synthesis by N₂ and Steam Electrolysis in Molten Hydroxide Suspensions of Nanoscale Fe₂O₃. *Science* **2014**, *345*, 637–640.
- (28) Li, F.-F.; Licht, S. Advances in Understanding the Mechanism and Improved Stability of the Synthesis of Ammonia from Air and Water in Hydroxide Suspensions of Nano-scale Fe₂O₃. *Inorg. Chem.* **2014**, *53*, 10042–10044.
- (29) Ingram, M. D.; Baron, B.; Janz, G. J. The Electrolytic Deposition of Carbon from Fused Carbonates. *Electrochim. Acta* **1966**, *11*, 1629–1639.
- (30) Ijije, H. V.; Lawrence, R. C.; Siambun, N. J.; Jeong, S. M.; Jewell, D. A.; Hu, D.; Chen, G. Z. Electro-deposition and Re-oxidation of Carbon in Carbonate-containing Molten Salts. *Faraday Discuss.* **2014**, *172*, 105–116.
- (31) Ida, J.; Lin, Y. S. Mechanism of High-temperature CO₂ Sorption on Lithium Zirconate. *Environ. Sci. Technol.* **2003**, *37*, 1999–2004.
- (32) Barin, I. Thermochemical Data of Pure Substances. 2008, DOI: 10.1002/9783527619825.
- (33) Website of National Institute of Standards and Technology, Link: <http://webbook.nist.gov/chemistry/>.
- (34) Kaplan, V.; Wachtel, E.; Lubomirsky, I. Conditions of Stability for (Li₂CO₃ + Li₂O Melts in Air. *J. Chem. Thermodyn.* **2011**, *43*, 1623–1627.
- (35) Novoselova, I. A.; Oliinyk, N. F.; Voronina, A. B.; Volkov, S. V. Electrolytic Generation of Nano-Scale Carbon Phases with Framework Structures in Molten Salts on Metal Cathodes. *Z. Naturforsch., A: Phys. Sci.* **2008**, *63*, 467–474.
- (36) Li, F.-F.; Lau, J.; Licht, S. Sungas instead of syngas: Efficient co-production of CO and H₂ with a single beam of sunlight. *Adv. Science* **2015**, DOI: 10.1002/advs.201500260.
- (37) Haber, F.; Tolloczko, S. *Z. Anorg. Allg. Chem.* **1904**, *41*, 412.
- (38) Cassir, M.; Moutiers, G.; Devynck, J. Stability and Characterization of Oxygen Species in Alkali Molten Carbonate: A Thermodynamic and Electrochemical Approach. *J. Electrochem. Soc.* **1993**, *140*, 3114–3123.
- (39) Frangini, S.; Scaccia, S. Sensitive Determination of Oxygen Solubility in Alkali Carbonate Melts. *J. Electrochem. Soc.* **2004**, *151*, A1251–A1256.